Supplemental material

Silverman et al., https://doi.org/10.1084/jem.20190009

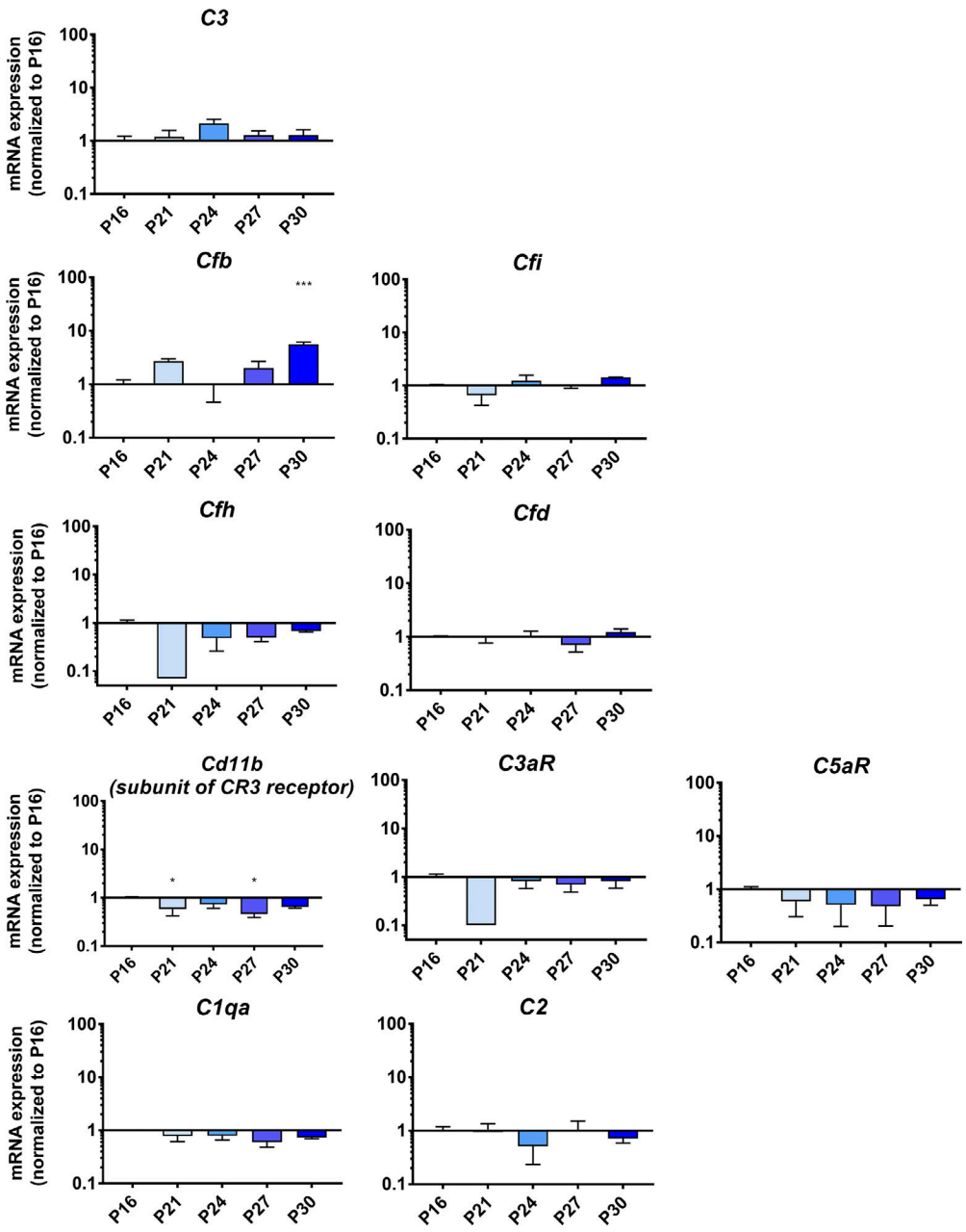

Figure S1. **Complement components, regulatory factors, and receptors are not markedly increased in expression in WT retina across the ages of P16 to P30.** mRNA expression levels of different complement components in WT retina analyzed using RT-PCR did not demonstrate patterns of prominent and sustained up-regulation comparable to those observed in rd10 retina during photoreceptor degeneration (P16 to P30). Expression levels for each gene at different time points were normalized relative to that at P16, P values for comparisons relative to levels at P16: *, P < 0.05; ***, P < 0.001; one-way ANOVA with Dunnett's multiple comparison test; *n* = 4 animals per time point; data collected from two independent experiments for each gene. All data shown as mean ± SEM.

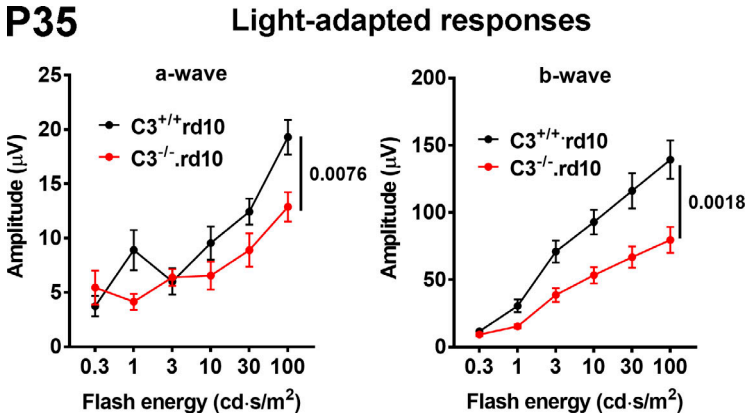

Figure S2. **C3 deficiency in the rd10 mouse model results in accelerated functional cone degeneration.** ERG evaluation at P35 at a later time point where cone degeneration is underway demonstrated decreased light-adapted, cone a- and b-wave amplitudes in $C3^{-/-}$.rd10 relative to $C3^{+/+}$.rd10 animals (P values were derived from a two-way ANOVA with Tukey's multiple comparisons test; number of eyes analyzed: $C3^{+/+}$.rd10 = 16; $C3^{-/-}$.rd10 = 14). Data collected from four independent experiments. All data shown as mean ± SEM.

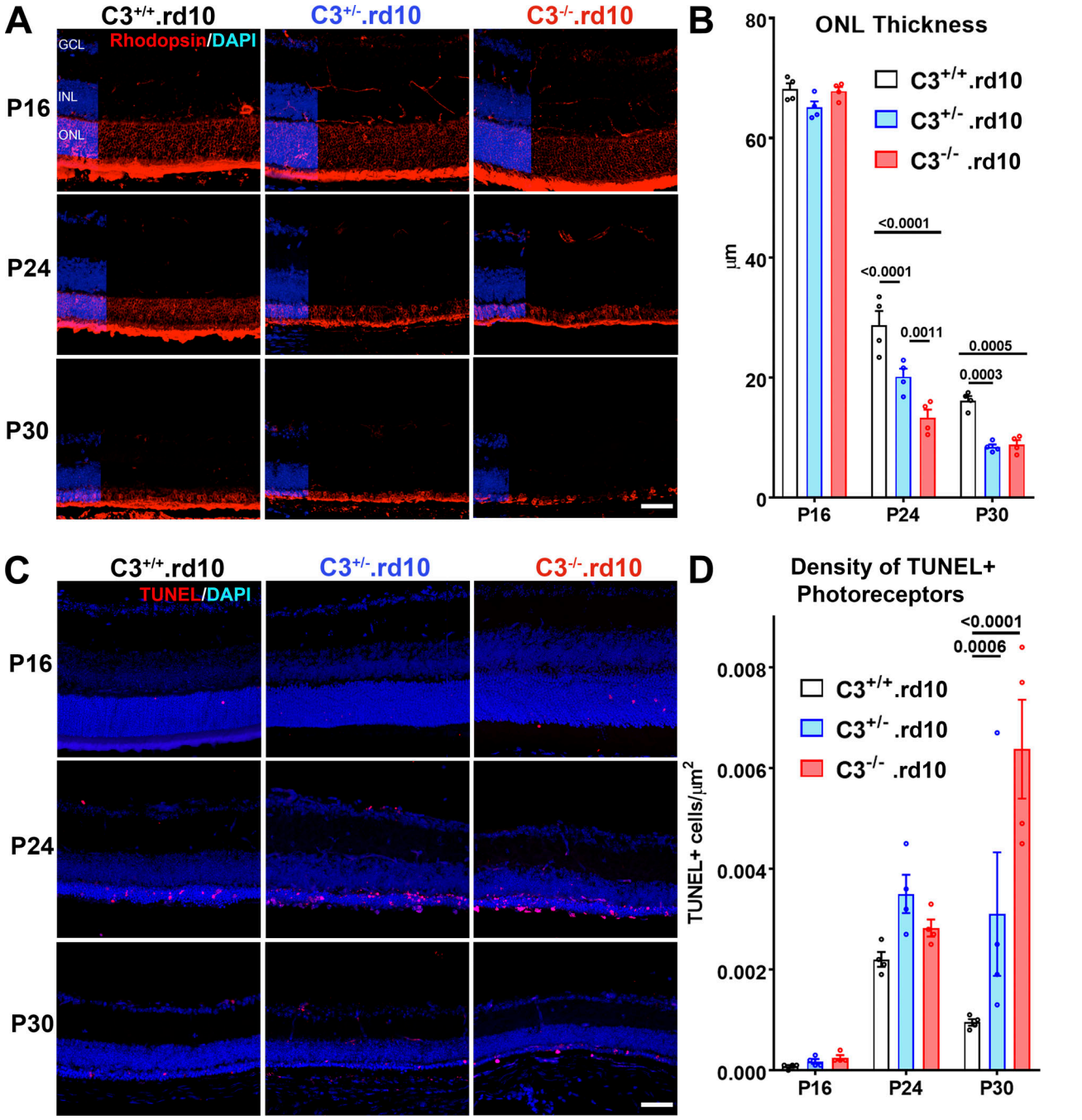

Figure S3. **Histological evidence of accelerated rod photoreceptor degeneration in C3 deficiency in the rd10 mouse model. (A and B)** The effects of C3 genotype on ONL thickness and rod photoreceptor degeneration were analyzed in retinal sections from $C3^{+/+}$.rd10, $C3^{+/-}$.rd10, and $C3^{-/-}$.rd10 animals at P16, P24, and P30. Retinal lamination and ONL thickness, as revealed by nuclear labeling with DAPI (blue), were similar between genotypes at P16. At P24 and P30, decreases in the thickness of the ONL layer were significantly greater in $C3^{+/-}$.rd10 and $C3^{-/-}$.rd10, relative to $C3^{+/+}$.rd10 animals. Immunohistochemical analysis of rhodopsin labeling (red) also demonstrated more severe shortening of rod outer segments and loss of rods in $C3^{+/-}$.rd10 and $C3^{-/-}$.rd10 animals. **(C and D)** Analysis of the density of TUNEL$^+$ apoptotic cells in the ONL showed minimal TUNEL labeling at P16 but significantly greater density in $C3^{+/-}$.rd10 and $C3^{-/-}$.rd10 animals relative to $C3^{+/+}$.rd10 animals. P values were derived from a two-way ANOVA with Tukey's multiple comparisons test; n = 4 animal per genotype and age group. Scale bars, 50 µm. Data collected from two independent experiments each. All data shown as mean ± SEM.

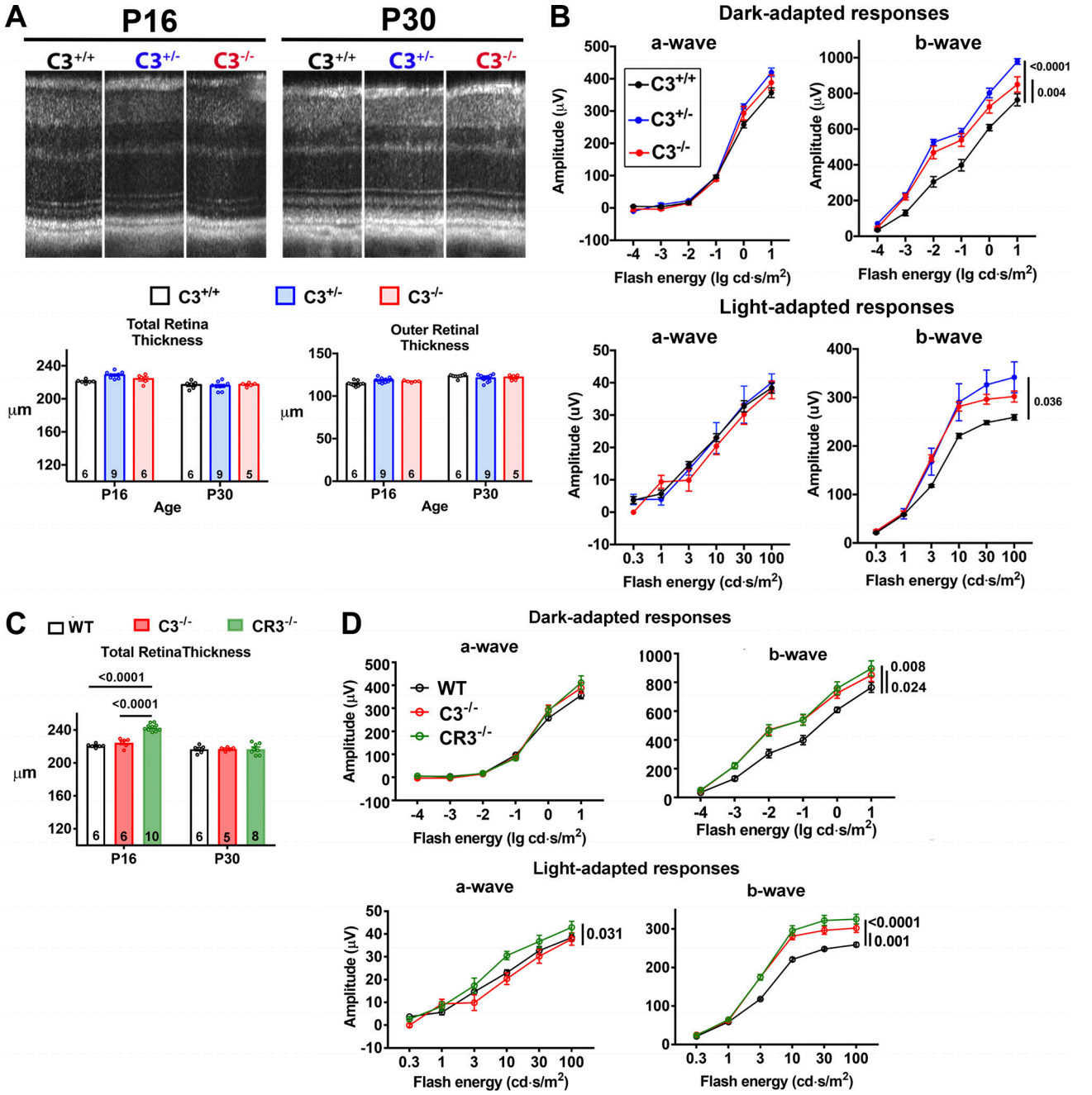

Figure S4. **Effect of C3 and CR3 genetic deficiency in the absence of the rd10 mutation on retinal thickness and ERG function. (A)** Retinal lamination and thickness of $C3^{+/+}$, $C3^{+/-}$, and $C3^{-/-}$ animals (in the absence of the rd10 mutation) were evaluated at P16 and P30 using in vivo OCT imaging. The nature of retinal lamination was similar between the three genotypes at both ages, and the total and outer retinal thicknesses were also statistically nondistinct. P values were derived from a two-way ANOVA with Tukey's multiple comparisons test; number of eyes analyzed in each group is provided at the bottom of each column. **(B)** ERG evaluation of retinal function at P24 showed no significant differences between the three genotypes with respect to dark- and light-adapted a-wave amplitudes, indicating similarities in both rod and cone photoreceptor functions. Dark- and light-adapted b-wave amplitudes were, however, slightly and significantly higher in $C3^{+/-}$ and $C3^{-/-}$ animals relative to $C3^{+/+}$ animals, indicating a deficit in synaptic elimination and refinement at the level of the OPL in C3 deficiency. P values were derived from a two-way ANOVA with Tukey's multiple comparisons test; number of eyes analyzed: seven, five, and five for $C3^{+/+}$.rd10, $C3^{+/-}$.rd10, and $C3^{-/-}$.rd10 animals, respectively. **(C)** Retinal thickness of WT, $C3^{-/-}$, and $CR3^{-/-}$ animals in the absence of the rd10 mutation were compared at P16 and P30 using in vivo OCT imaging. Total retinal thicknesses were greater in $CR3^{-/-}$ relative to the other two genotypes at P16 but were statistically similar between all three genotypes at P30. P values were derived from a two-way ANOVA with Tukey's multiple comparisons test; number of eyes analyzed in each group is provided at the bottom of each column. **(D)** ERG evaluation of dark-adapted retinal function at P24 showed that $CR3^{-/-}$ animals showed similar a-wave amplitudes but increased b-wave amplitudes relative to WT animals, matching those in $C3^{-/-}$ animals. Light-adapted ERG evaluation showed a slight a-wave amplitude increase in $CR3^{-/-}$ animals relative to the other two genotypes, while b-wave amplitudes in $CR3^{-/-}$ animals were higher than those in WT animals, matching those found in $C3^{-/-}$ animals. P values were derived from a two-way ANOVA with Tukey's multiple comparisons test; number of eyes analyzed: seven, five, and six for WT, $C3^{-/-}$, and $CR3^{-/-}$ animals, respectively. Data collected from three independent experiments in $C3^{-/-}$ and $CR3^{-/-}$ mice. All data shown as mean ± SEM.

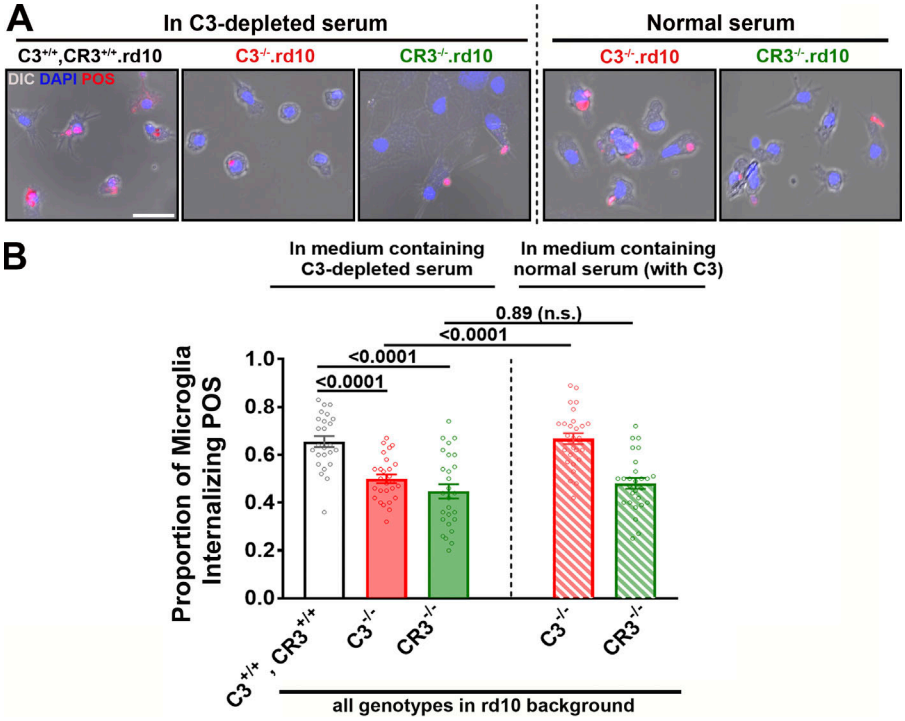

Figure S5. **In vitro C3 opsonization of POSs mediates their phagocytosis by microglia via a C3-CR3–dependent mechanism.** Phagocytic capacities of microglia isolated from P24 $C3^{+/+}$, $CR3^{+/+}$.rd10, $C3^{-/-}$.rd10, and $CR3^{-/-}$.rd10 retinas were evaluated in an in vitro phagocytic assay that assessed the phagocytic uptake of bovine rod POSs added in culture. **(A)** Fluorescently labeled POSs (red) were incubated with cultured microglia (seen in differential interference contrast images) in the presence of either in normal, C3-sufficient, or C3-depleted serum and cultured for 2 h to permit microglial phagocytosis. Scale bar, 25 µm. **(B)** Under C3-depleted conditions, the proportions of $C3^{-/-}$.rd10 and $CR3^{-/-}$.rd10 microglia phagocytosing POS were similar and significantly lower than that in $C3^{+/+}$, $CR3^{+/+}$.rd10 microglia, indicating a requirement for microglial production of C3 and expression of CR3 for POS phagocytosis. However, in a medium containing extracellular C3, the proportion of POS^{+} $C3^{-/-}$.rd10 microglia was significantly increased to the level demonstrated by $C3^{+/+}$, $CR3^{+/+}$.rd10 microglia, indicating that exogenous C3 can compensate for the absence of microglia-derived C3. Exogenous C3 did not increase the phagocytic rate in $CR3^{-/-}$.rd10 microglia, indicating a maintained requirement for microglial CR3 function. P values were derived from a one-way ANOVA with Tukey's multiple comparisons test; n = 24–26 replicates per condition; data collected from two independent experiments. All data shown as mean ± SEM.

Table S1. **List of primers used for RT-PCR reactions**

Gene	Forward (5′–3′)	Reverse (5′–3′)
C1qa	CAAGGACTGAAGGGCGTGAA	CAAGCGTCATTGGGTTCTGC
C2	CTCATCCGCGTTTACTCCAT	TGTTCTGTTCGATGCTCAGG
C3	GAAGTACCTCATGTGGGGCC	CAGTTGGGACAACCATAAACC
C3 (exon 4)	AATGTCTGCCTTCTCTACCACATC	GTGAAGGGTGACCCAAGAGATAAC
C3aR	GGAAGCTGTGATGTCCTGG	CACACATCTGTACTCATATTGT
C5aR	GAGGGTGGAGAAGCTGAAC	CTACACCGCCTGACTCTTC
Cfb	GAGGATGGGCACAGCCCAG	GACCATATCGTGGCCTCACC
Cfd	GCAGAGAGCAACCGCAGG	CAGGATGTCATGTTACCATTTG
Cfh	CTTACATGCATGTGTAATACCA	TTATACACAAGTGGGATAATTGA
Cfi	CCATTGATGCCTGCAAAGGA	CAGACATTGTGTTGAGAAACAA
Cd11b	GCAGGAGTCGTATGTGAGG	TTACTGAGGTGGGGCGTCT
Cd11b (exon 1)	TAGAGGGCACCTGTCTGGTTA	GACTCTTAAAGCTCTTCTGGTCACA